ORGANIC LETTERS

2004
Vol. 6, No. 6
877−880

Cause of Hydration/Dehydration in Condensed Organic Materials: Synthesis of Hydrophobic Pores

Martín Febles,[†] Cirilo Pérez,*,[†] Concepción Foces-Foces,[‡] Matías L. Rodríguez,*,[†] Natalia Pérez-Hernández,[§] Ezequiel Q. Morales,[§] and Julio D. Martín*,[§]

Instituto de Bioorgánica, Universidad de La Laguna, CSIC, Ctra. Vieja de la Esperanza, 2, 38206 La Laguna, Tenerife, Spain, Instituto de Química-Física Rocasolano, CSIC, Serrano 119, E-28006 Madrid, Spain, and Instituto de Investigaciones Químicas, CSIC, Américo Vespucio, s/n, Isla de la Cartuja, 41092 Seville, Spain

jdmartin@iiq.csic.es

Received December 1, 2003

ABSTRACT

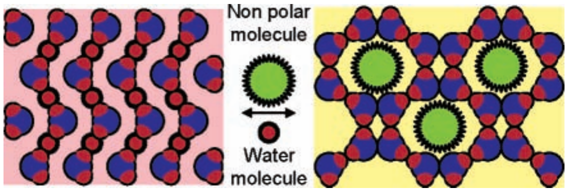

The unique solid-state hydration/dehydration properties of the diacid (±)-1e in comparison with other homologues of the same family are studied. Hydrophobic enhancement, which is a consequence of the loss of water molecules from (±)-1e chains, is a property that can be exploited to achieve organic condensed systems for nonpolar molecules by interstitial van der Waals confinement.

Since the inclusion of water molecules in H-bonded organic aggregates is a reversible process that exhibits slow kinetics of nucleation and crystal growth;[1] in optimized states, it can be expected that both hydrated and anhydrous nuclei structures should initially coexist in equilibrium. At some turning point during crystallization the energy barrier among hydrated/anhydrous molecular arrangements suddenly goes from low (solution) to high (crystalline phase), and the crystal structure becomes locked into one particular kind of symmetric arrangement.[2] This is an important point of reference in regard to our research, which is aimed at understanding the interplay between water molecules and organic systems.[3] To this end, we designed amphiphilic molecules where one property is varied while the others are kept constant to ascertain whether or not their aggregations would exhibit water association. On the basis this approach, we have recently published the solid-state hydration behavior of a family of dicarboxylic acids of general structure **(±)-1**[4] (Figure 1) by slow crystallization from the H_2O/CCl_4 interface.

Although the molecular basis for maintaining hydrated patterns is unclear, it appears that a quasispherical molecular shape is required. The protrusions caused by the cyclopropyl

---

[†] Instituto de Bioorgánica.

[‡] Instituto de Química Física.

[§] Instituto de Investigaciones Químicas.

(1) (a) Eisenberg, D.; Kauzmann, W. *The Structure and Properties of Water*; Oxford University Press: New York, 1969. (b) Robinson, G. W.; Zhu, S.-B.; Singh, S.; Evans, M. W. *Water in Biology, Chemistry, and Physics*; World Scientific; Singapore, 1996.

(2) Gavezzoti, A. *Synlett* **2002**, 201−214.

(3) (a) Pérez, C.; Espínola, C. G.; Foces-Foces, C.; Núñez-Coello, P.; Carrasco, H.; Martín, J. D. *Org. Lett.* **2000**, *2*, 1185−1188. (b) Carrasco, H.; Foces-Foces, C.; Pérez, C.; Rodríguez, M. L.; Martín, J. D. *J. Am. Chem. Soc.* **2001**, *123*, 11970−11981.

(4) The model includes a variable-in-size van der Waals site and fixed H-bonding functions. Hence, hydration is driven by cooperation between these two well-defined interactions sited over two distinct zones of the model. Slow crystal nucleation and growth from the H_2O/CCl_4 interface gave hydrated arrays in three (**1e**−**g**) of the seven molecules studied. The four bulkier homologues (**1a**−**d**) generated anhydrous structures. Pérez, C.; Rodríguez, M. L.; Foces-Foces, C.; Pérez-Hernández, N.; Pérez, R.; Martín, J. D. *Org. Lett.* **2003**, *5*, 641−644.

10.1021/ol036335d CCC: $27.50

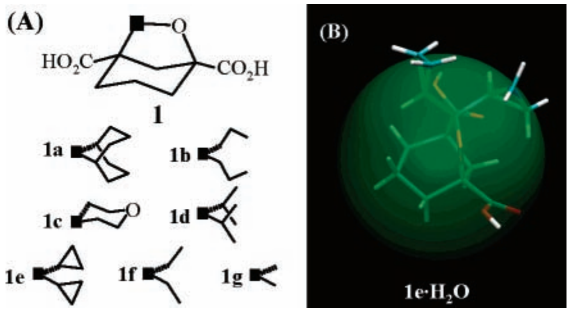

Figure 1. (A) Family of diacids used in this study. (B) Capped-stick representation of **1e**·H_2O. The transparent green sphere is included to emphasize the spherical geometry (radius = 3.9 Å).

appendages of compound **1e** are within the limit of the maximal deviation allowed from ideal spherical geometry. Larger appendages provide anhydrous packing.[4] In this sense, the possibility of lattice waters thrice-coordinated to discrete sites for the frontier homolog **1e** may provide a nice and simple benchmark for direct test causes of hydration as a compensation between dynamics and binding.[5]

We report here that compound (±)-**1e** does not follow the trend of its larger or smaller homologues, which retain their crystal behavior unaltered by dissolution and re-growth under variable aqueous/organic interfaces and conditions. For instance, compound (±)-**1e** gave anhydrous crystals after undergoing slow crystallization from H_2O/CCl_4 under methane or ethane at atmospheric pressure. Thus, (±)-**1e** is capable of being efficiently packed in the 1:1 hydrated A_1 phase,[4] or anhydrous B_1, B_2 (methane), and B_3 (ethane) phases, a fact not observed in its smaller (**1f**−**g**) or larger (**1a**−**d**) homologues.[6] The underlying reasons for this phenomenon are discussed below and the impact on the operation of the crystallization process is highlighted.

A reasonable cause for the hydration of (±)-**1e** can be hypothesized by simply comparing the three-dimensional structures of the anhydrous (B_1, B_2, B_3) and hydrated (A_1) phases. Thus, the anhydrous B_1 phase, triclinic, consists of the classical carboxylic acid $R_2^2(8)$ dimer motif of (±)-**1e** molecules forming extended chains. Interchain indentation occurs, manifesting an enhancement of van der Waals interactions in a similar way to its homologues of larger size (**1a**−**d**).[4] However, in contrast with the latter, the B_1 phase exhibits solid-to-solid phase transition when decreasing the temperature from 300 to 170 K. The transition consists of the change of conformation of one cyclopropyl appendage, which is disordered at temperatures higher than 220 K. Therefore, the volume thermal expansion is positive.[7]

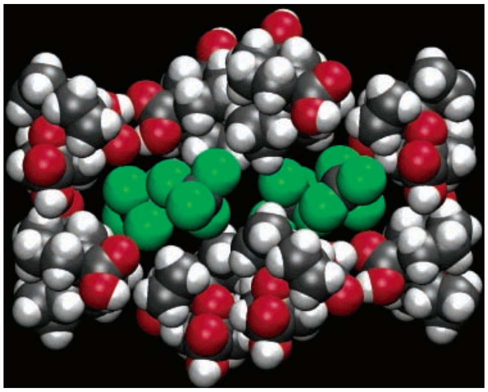

Figure 2. Space-filling representation of the (±)-**1e**·CCl_4 (B_3 phase) structure, showing a cross section through one pore as a projection in the *ab* plane. The projection shows how the cyclopropyl appendages are directed toward the center of the pore. Disordered carbon tetrachloride molecules occupy the pore interior. Color code: H, white; C, gray; O, red; and Cl, green.

Phase B_2, triclinic, obtained by crystallization of (±)-**1e** under methane, formed an H-bonded array where two independent molecules of **1e**, plus those centrosymmetrically related, created $R_4^4(26)$ rings which are connected through carboxy dimers in the classical $R_2^2(8)$ motif, forming skewed capsules, each with an estimated accessible volume[8] of 200 $Å^3$. One methane molecule remained trapped in the interstitial lattice cavity, although a reasonable model incorporating methane could not be properly elucidated because of the high guest disorder. To probe the cavity size, we prepared crystals of the $CHCl_3$ and CH_2Cl_2 solvates by slow evaporation of a solution (±)-**1e** in CCl_4/H_2O to which $CHCl_3$ or CH_2Cl_2 was added. The crystal structures of the complexes, thus obtained, are pseudoisomorphous with the previous one and the interstitial cavity is occupied by one molecule of $CHCl_3$ or two molecules of CH_2Cl_2. Owing to the scantly constricted environment (partial PE, 0.63, CH_4; 0.62, CH_2Cl_2; 0.61 $CHCl_3$) guest molecules remain disordered and only van der Waals contacts occur between host and guest atoms.

Phase B_3, monoclinic, obtained by crystallization under ethane, forms chains of (±)-**1e** molecules via the carboxy dimer H-bonding motif. The most important feature of this structure is that centrosymmetrical chains leave channels along the crystallographic *a* axis. The minor axis of the elliptical section (12.7 × 6.9 Å) at $a = 0$ decreases in the *c* direction from $a = 0$ to $^1/_4$ where it blocks the center due to the protrusions caused by cyclopropyl appendages. Then, it gradually reopens until the full width is restored, that is, at a repetition length of $a/2 \approx 4.0$ Å. The channels, which are estimated to be approximately 50% of the total volume (partial PE, 0.47), are filled with disordered carbon tetrachloride guest molecules (Figure 2). The crystal shows spongelike dynamic behavior.[9] It appears that, prior to carbon tetrachloride inclusion, volatile ethane molecules template the highly porous arrangement.

---

(5) The hydration cost has more to do with the number of water H bonds than with their strength. Hence, the closer water is to an aqueous/organic interface transition, the stronger the expected hydrophobic assembly. For an experimental study that probes the weakness of water H bonding at H_2O/CCl_4 and H_2O/hydrocarbon interfaces, see: Scatena, L. F.; Brown, M. G.; Richmond, G. L. *Science* **2001**, *292*, 908−912.

(6) Slow crystallization from a variety of H_2O/nonpolar organic solvent interfaces under methane or ethane atmosphere of compounds (±)-**1a**−**g** reproduces previously reported packing,[4] with the sole exception of (±)-**1e**, which gave anhydrous crystals.

These observed packing divergences for compound **1e** can be assumed by considering their hydrated and anhydrous phases to be "frozen" molecular arrangements, otherwise in equilibrium. The increase of molecular volume in B_1**,** or the inclusion of nonpolar molecules in the B_2 and B_3 phases, is due to the hydrophobic enhancement caused by a loss of water molecules as a compensation of the thermodynamic parameters of hydrated/anhydrous aggregation stages in equilibrium.[10] Thus, to the extent to which hydrated molecules increase their bonding (ΔH decrease) their motions will decrease (ΔS decrease), and their relative intermolecular distances will also decrease (ΔV decrease) and vice versa. Furthermore, this example shows that evaporation of water molecules in the vicinity of extended H-bonded chains provides the driving force to stabilize critical clusters of hydrophobic guests by chain folding[11] (Figure 3).

In conclusion, the model illustrates how the assembly of hydrophobic moieties is enhanced by removal of water molecules from regions between these groups. As observed with biological macromolecules,[12] the hydrophobic stabilization of small amphiphilic molecules is also more favorable than the entropic cost of maintaining the offset in hydrated systems, and is therefore cause for segregation of water molecules from H-bonded arrays. Since anisotropic dipolar molecules are expected to nucleate in single chains,[13] it is during subsequent self-assembly to 2D and 3D clusters that the traditional Kauzmann-type hydrophobicity can appear.[12] This time-sequenced process validates the model aimed at identifying single parameters and functions in order to study, at the atomic level, the strength of the hydrophobic effect. Moreover, the consequence of the loss of water molecules by hydrophobic volatile templates is a property that can be exploited for producing porous crystalline structures.

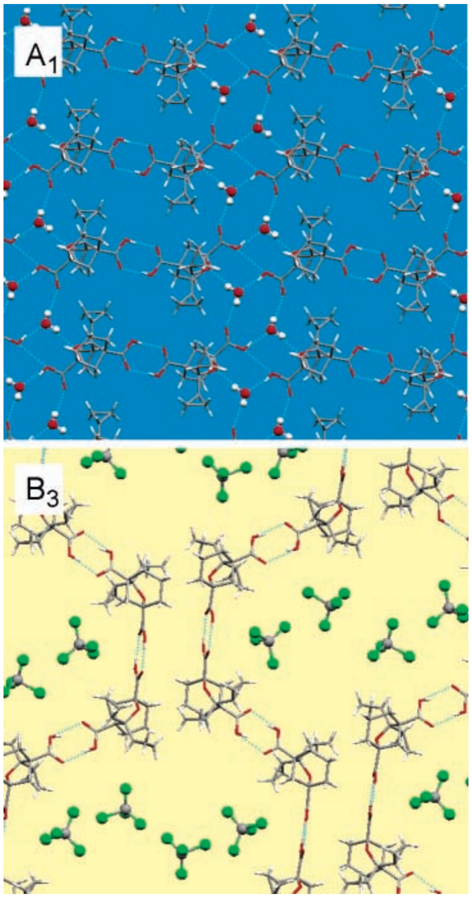

Figure 3. Differences in packing (capped-stick representation) between hydrated (A_1) and anhydrous (B_3) phases. A_1, crystal packing of (±)-**1e** molecules forming interconnected H-bonded chains. B_3, crystal packing of (±)-**1e** molecules under an atmosphere of ethane. Anhydrous chains folding to create centrosymmetric octamers that form elliptical channels which are filled with carbon tetrachloride molecules. Different background colors mark the differences of the local dielectric constant and hence the electrostatic field within chains: hydrophilic (A_1, pale blue) and hydrophobic (B_3, pale yellow). Ball-and-stick representation of water (A_1) and carbon tetrachloride (B_3) molecules. Colors are as follows: C, gray; O, red; Cl, green; and H, white. Dotted cyan lines represent OH···O hydrogen bonds.

We have reported[3] how water-induced nucleation processes might create pores which exhibit hydrophilic behavior. The model studied here intrinsically indicates that enhancement of the hydrophobic effect to give porous materials, manifested by an accommodated refill of the pore with disordered CH_4, CH_2Cl_2, $CHCl_3$, or CCl_4 molecules, in preference to water, is caused by an effective dehydration event at earlier nucleation stages.[14]

Acknowledgment. This work was supported by the Spanish DGICyT (Grant BQU2001-1137). M.F. and N.P.H. thank the Spanish Ministry of Science and Technology for a Predoctoral Fellowship.

---

(7) Crystals of the B_1 phase show reversible phase transition in the 220−200 K interval maintaining the crystalline state during and after the transition. Diffraction measurements were collected at 300 and 170 K. The cell constants *a*, *b*, and *c* are elongated as the temperature increases while the α and *β* angles increase and decrease, respectively. The significant increase in cell volume at 300 K (730.8(2) vs 705.5(1) $Å^3$) results in the disorder of one cyclopropyl appendage, which also changes its conformation with respect to that of the low-temperature phase (Supporting Information).

(8) Accessible volume means that which can be accessed by a given probe from outside the crystal. This was calculated with a 1.4 Å probe, using VMD version 1.8.1. (Humphrey, W.; Dalke, A.; Schulten, K. *J. Mol. Graphics* **1996**, *14.1*, 33−38).

(9) Work to establish crystal-to-crystal transformation upon the removal of the nonpolar guest and exchange processes is currently under way.

(10) (a) Williams, D. H.; O'Brien, D. P.; Bardsley, B, *J. Am. Chem. Soc.* **2001**, *123*, 737−738. (b) Searly, M. S.; Williams, D. H. *J. Am. Chem. Soc.* **1992**, *114*, 10690−10697.

(11) For a recent computer simulation study see: ten Wolde, P. R.; Chandler, D. *Proc. Natl. Acad. Sci. U.S.A.* **2002**, *99*, 6539−6543.

(12) (a) Kauzmann, W. *Adv. Protein Chem.* **1959**, *14*, 1−63. (b) Tanford, C. *The Hydrophobic Effect*: *Formation of Micelles and Biological Membranes*, 2nd ed.; Wiley Interscience: New York, 1980. (c) Dill, K. A. *Biochemistry* **1990**, *29*, 7133−7155. (d) Tanford, C. *Protein Sci.* **1997**, *6*, 1358−1366. (e) Lazaridis, T. *Acc. Chem. Res.* **2001**, *34*, 931−937.

(13) (a) ten Wolde, P. R.; Frenkel, D. *Science* **1997**, *277*, 1975−1978. (b) ten Wolde, P. R.; Oxtoby, D. W.; Frenkel, D. *Phys. Rev. Lett.* **1998**, *81*, 3695−3698. (c) Talenquer, V.; Oxtoby, D. W. *J. Chem. Phys.* **1998**, *109*, 223−227.

(14) For recent examples of organic porous materials, see: (a) Amorin, M.; Castedo, L.; Granja, J. R. *J. Am. Chem. Soc.* **2003**, *125*, 2844−2845. (b) Alshahateet, S. F.; Bishop, R.; Craig, D. C.; Scudder, M. L. *CrystEngComm* **2002**, *8*, 1−4. (c) Tanaka, T.; Tasaki, T.; Aoyama, Y. *J. Am. Chem. Soc.* **2002**, *124*, 12453−12462. (d) Nangia, A. *Curr. Opin. Solid State Mater. Sci.* **2001**, *5*, 115−122. (e) Aoyama, Y. *Top. Curr. Chem.* **1998**, *198*, 131−161. (f) Russell, V. A.; Evans, C. C.; Li, W.; Ward, M. D. *Science* **1997**, *276*, 575−579.

Supporting Information Available: Crystallization experiments, crystallographic tables, atomic coordinates, and thermal parameters, and selected bond lengths and angles for anhydrous structures (B1, B2, and B3 phases) of **(±)-1e** and X-ray crystallographic files. This material is available free of charge via the Internet at http://pubs.acs.org.

OL036335D